Cell Reports, Volume *24*

Supplemental Information

Neuronal Mitochondrial Dysfunction Activates the Integrated Stress Response to Induce Fibroblast Growth Factor 21

Lisa Michelle Restelli, Björn Oettinghaus, Mark Halliday, Cavit Agca, Maria Licci, Lara Sironi, Claudia Savoia, Jürgen Hench, Markus Tolnay, Albert Neutzner, Alexander Schmidt, Anne Eckert, Giovanna Mallucci, Luca Scorrano, and Stephan Frank

SUPPLEMENTARY EXPERIMENTAL PROCEDURES

Mice. Generation of tamoxifen-inducible, forebrain neuron-specific Drp1$^{flx/flx}$ Cre^{+} mice was described recently (Oettinghaus et al., 2016). At 8 weeks of age recombination of the floxed loci was induced by tamoxifen injection (Sigma Aldrich, Germany; 1mg twice daily for 5 consecutive days). For genotyping, genomic DNA was isolated from tail tips by proteinase K digestion (Sigma Aldrich, Germany). CreERT2 transgene was amplified using the following primers: 5' GGT TCT CCG TTT GCA CTC AGG A 3', 5' CTG CAT GCA CGG GAC AGC TCT 3', 5' GCT TGC AGG TAC AGG AGG TAG T 3'. Recombination of the Drp1 locus was detected using the following primers: 5' CAG CTG CAC TGG CTT CAT GAC TC 3', 5' TGC CAA GAA TGA TTA CAG TCA GG 3'.

Mutant tau (P301L) and prion-injected (RML) mice have been described elsewhere (Moreno et al., 2013; Radford et al., 2015). When indicated, mice were treated orally with PERK inhibitor GSK2606414 (50mg/kg, three doses, starting at 10 wpi; Moreno et al., 2013).

For intraventricular tunicamycin microinjections, mice were anaesthetized by i.p. injection of 10 mg/kg ketamine and 20 mg/kg xylazine. Injections were performed with a 10 µl Hamilton microsyringe as described (Ono et al., 2012) using -0.5 mm posterior, -1.0 mm lateral, -2.0 mm inferior relative to bregma as coordinates. 2 µl of 0.1 µg/µl tunicamycin in 1% DMSO or 2 µl vehicle were carefully injected over the course of 2 min and the needle left in place for 5 min before retraction. Following scalp suture mice were monitored until recovery from anesthesia. After 48h, mice were sacrificed, their hippocampi dissected and plasma collected (between 9 and 10 AM).

TUDCA treatment was initiated at day 1 PTI. Mice were fed 0.4% TUDCA-supplemented chow (chow: ssniff, Germany; TUDCA: Merck, UK) for 7 weeks.

All experiments were performed under specific pathogen-free conditions, in accordance with Swiss animal protection legislation and with approval of the Basel Veterinary Committee for Animal Care (permits 2393, 23288).

Western Blot. Lysates of perfused mouse brains were analyzed as previously described (Oettinghaus et al., 2016). Membranes were probed with the following antibodies: Drp1 (BD Biosciences; 611112), Atf4 (Santa Cruz; sc-200), Bip (BD Biosciences; 610978), eIF2α total (Cell Signaling Technology, #5324), eIF2α phospho-Ser51 (Cell Signaling Technology, #3398), Hsp60 (Enzo; ADI-SPA-807-E), actin (Thermo

Scientific; MA1-91399), GAPDH (Abnova; H00002597-M03) and beta-tubulin (Sigma; T8660). Secondary antibodies were anti mouse-HRP (GE Healthcare; NA931) and anti-rabbit-HRP (GE Healthcare; NA934); for signal detection Amersham ECL Prime Western Blotting Detection Reagent (GE Healthcare; RPN2232) was used in conjunction with Amersham Hyperfilm (GE Healthcare; 28-9068-44), or with an Azure C300 imager (Azure Biosystems, USA). Densitometry was performed using ImageJ.

Histology and immunohistochemistry. Following transcardial formaldehyde perfusion of anaesthetized mice, histological assessment was performed using previously described protocols (Oettinghaus et al., 2016).

In brief, coronal hippocampal sections (4 μm) were prepared from formalin-fixed, paraffin-embedded (FFPE) wildtype mouse brain and hematoxylin-eosin stained using standard protocols. In addition, FFPE sections were subjected to immunohistochemistry using anti-GFAP (DAKO; 1:500), anti-NeuN (Chemicon; 1:200), and anti-Iba1 (Wako; 1:3000); secondary antibody was anti-rabbit IgG (Vector; ImmPRESS Reagent Kit). All immunohistochemical stains were performed on an automated Ventana immunostaining instrument using prediluted antibodies (Ventana Medical Systems Inc.).

Fluorescent detection of Fgf21 mRNA. This analysis was performed as a service by Advanced Cell Diagnostics, Inc. with the RNAscope technology, following standard manufacturer's protocol. Briefly, frozen mouse brain sections (10μm) were stained with probes targeting Fgf21, Aldh1l1 (astrocytes) and RBfox3 (also known as NeuN, neurons) mRNAs. POLR2A/PPIB/UBC were used as a positive control marker for sample quality control and to evaluate RNA quality in both tissue samples. Bacterial gene dapB was used as a negative control. Images were acquired on a Zeiss LSM 510 Meta confocal microscope.

For quantification of Fgf21 signal, Fgf21-positive area/ total area was employed within the CA1 region. Briefly, images were thresholded and analyzed with the "analyze particles" function on ImageJ within an indicated ROI corresponding to the CA1 region.

Ultrastructural analyses. Transmission electron microscopy was performed as previously described (Oettinghaus et al., 2016) using a Phillips CM100 transmission electron microscope.

Real-time PCR. Organs were collected from PBS-perfused mice and RNA was isolated (RNeasy Lipid Tissue Kit for adipose tissue, 74804; RNeasy Fibrous Tissue kit for muscle, 74704; RNeasy kit for other organs, 74104; all from Qiagen). Reverse-transcriptase PCR was performed using the High Capacity cDNA Reverse Transcription Kit (Invitrogen; 4368814). Real-time PCR was performed using TaqMan assays (Life Technologies) on a 7900HT Real-Time PCR System (Applied Biosystems). The following Taqman assays were used: FGF21 (Mm00840165_g1), 18S (Mm03928990_g1), Chop (Mm01135937_g1), PPARα (m00440939_m1), PPARδ (Mm00803184_m1), PGC-1α (Mm01208835_m1), PGC-1β (Mm00504720_m1), ATF4 (Mm00515325_g1), Akt1 (Mm01331626_m1), PI3K (Mm00803160_m1), Hsp10 (Mm00434083_m1), Clpp (Mm00489940_m1), Yme1l1 (Mm00496843_m1). Cross-threshold (ct) values were normalized to 18S ct values.

ELISA and other kits. Blood was collected between 9 and 10 AM in EDTA-coated tubes and hormone levels were detected by ELISA from plasma (FGF21: BioVendor, RD291108200R). Total amino acids were measured on hippocampi, cortices and cerebella 10 weeks PTI with the L-Amino Acid Quantitation Kit (MAK002, Sigma Aldrich, Germany) according to manufacturer's instructions.

Proteomics. In Fig. S2B, P-values denote likelihood of protein group being a random sample of the total population of detected proteins (Fisher's exact test). Reference dataset was obtained from (Han et al., 2013).

SUPPLEMENTARY FIGURE LEGENDS

Fig. S1 Cytoarchitecture of hippocampal pyramidal layer, related to Fig. 1C

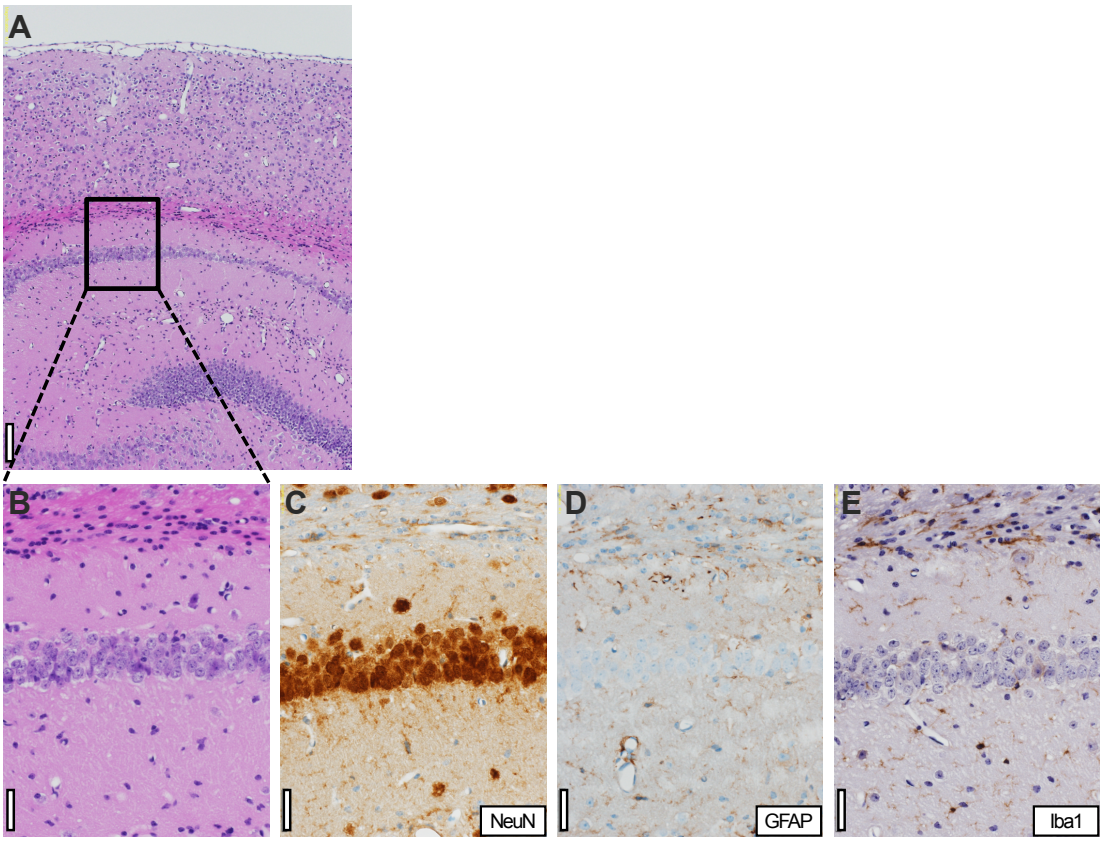

(A-E) Coronal cross-sections of hippocampal CA1 region stained with hematoxylin/eosin (A, B) or probed by immunohistochemistry for NeuN (C; neuronal), GFAP (D; astroglia), and Iba1 (E; microglia). Scale bars: 50μm (A), 20μm (B-E)

Fig. S2 Atf4 expression and target gene activation in Drp1-ablated brains, related to Fig. 1E-H

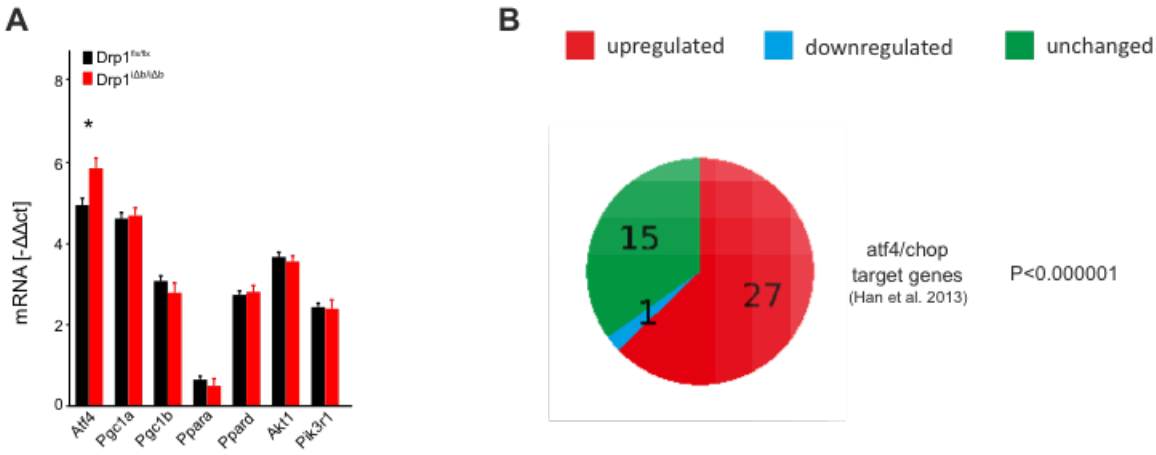

(A) mRNA expression in Drp1-ablated and control animals at 10 weeks PTI, normalized against 18S rRNA ct values. Data represent average ±SEM of at least 4 animals.

(B) Pie chart representing frequency distribution of up- and downregulated proteins of Drp1-ablated forebrain compared to wild-type brain.

Fig. S3 The mitochondrial UPR is not activated in Drp1-ablated brains, related to Fig. 3F-H

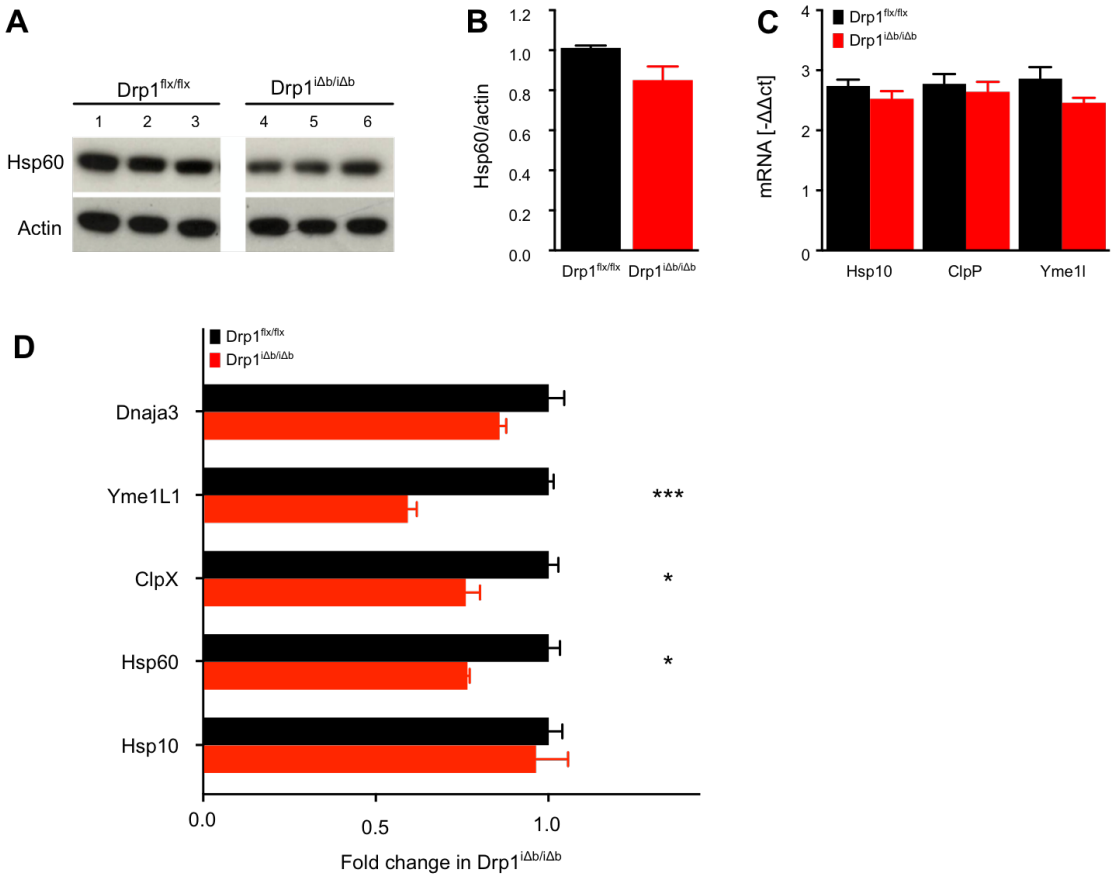

(A, B) Protein expression of mtUPR marker Hsp60 as determined by Western blot on hippocampal lysates at 10 weeks PTI, normalized to actin. Data represent average ±SEM of at least 4 animals.

(C) Hippocampal mRNA expression of *Hsp10*, *ClpP*, and *Yme1l* 10 weeks PTI as determined by qRT-PCR, normalized to 18S rRNA ct values. Data represent average ±SEM of at least 4 animals.

(D) Fold change in selected, mtUPR-related hits of a total proteomics screen 10 weeks PTI.

Asterisks in (D) denote q-values (i.e. p-values adjusted for multiple testing): *: $p<0.05$, ***: $p<0.001$.

SUPPLEMENTARY REFERENCES

Han, J., Back, S., Hur, J., Lin, Y., Gildersleeve, R., Shan, J., Yuan, C., Krokowski, D., Wang, S., Hatzoglou, M., et al. (2013). ER-stress-induced transcriptional regulation increases protein synthesis leading to cell death. Nat. Cell Biol. *15*, 481–490.

Moreno, J., Halliday, M., Molloy, C., Radford, H., Verity, N., Axten, J., Ortori, C., Willis, A., Fischer, P., Barrett, D., et al. (2013). Oral treatment targeting the unfolded protein response prevents neurodegeneration and clinical disease in prion-infected mice. Sci. Transl. Med. *5*, 206ra138.

Oettinghaus, B., Schulz, J., Restelli, L., Licci, M., Savoia, C., Schmidt, A., Schmitt, K., Grimm, A., Morè, L., Hench, J., et al. (2016). Synaptic dysfunction, memory deficits and hippocampal atrophy due to ablation of mitochondrial fission in adult forebrain neurons. Cell Death Differ. *23*, 18–28.

Ono, Y., Shimazawa, M., Ishisaka, M., Oyagi, A., Tsuruma, K., and Hara, H. (2012). Imipramine protects mouse hippocampus against tunicamycin-induced cell death. Eur. J. Pharmacol. *696*, 83–88.

Radford, H., Moreno, J., Verity, N., Halliday, M., and Mallucci, G. (2015). PERK inhibition prevents tau-mediated neurodegeneration in a mouse model of frontotemporal dementia. Acta Neuropathol. *130*, 633–642.